Flinders UNIVERSITY

Accepted Manuscript

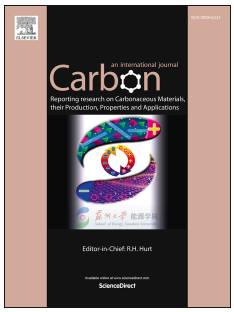

Shear stress mediated scrolling of graphene oxide

Thaar M.D. Alharbi, David Harvey, Ibrahim K. Alsulami, Nazila Dehbari, Xiaofei Duan, Robert N. Lamb, Warren D. Lawrance, Colin L. Raston

PII: S0008-6223(18)30500-1

DOI: 10.1016/j.carbon.2018.05.040

Reference: CARBON 13167

To appear in: *Carbon*

Received Date: 5 March 2018

Revised Date: 16 April 2018

Accepted Date: 20 May 2018

Please cite this article as: T.M.D. Alharbi, D. Harvey, I.K. Alsulami, N. Dehbari, X. Duan, R.N. Lamb, W.D. Lawrance, C.L. Raston, Shear stress mediated scrolling of graphene oxide, *Carbon* (2018), doi: 10.1016/j.carbon.2018.05.040.

Shear stress mediated scrolling of graphene oxide

Thaar M. D. Alharbi[1, 2], David Harvey [1], Ibrahim K. Alsulami [1], Nazila Dehbari [1], Xiaofei Duan [3], Robert N. Lamb [3], Warren D. Lawrance [1], Colin L Raston [1*]

[1] Flinders Centre for NanoScale Science & Technology, College of Science and Engineering, Flinders University, Adelaide SA 5001, Australia

[1]College of Science and Engineering, Flinders University, Adelaide SA 5001, Australia

[2] Physics Department, Faculty of Science, Taibah University, Almadinah Almunawarrah, Saudi Arabia

[3] School of Chemistry, TrACEES Platform, The University of Melbourne, Parkville, VIC 3010, Australia

[*]Corresponding author:

Tel: +61 8 82017958 E-mail address: colin.raston@flinders.edu.au (Colin Raston)

Abstract

Graphene oxide scrolls (GOS) are fabricated in high yield from a colloidal suspension of graphene oxide (GO) sheets under shear stress in a vortex fluidic device (VFD) while irradiated with a pulsed laser operating at 1064 nm and 250 mJ. This is in the absence of any other reagents with the structure of the GOS established using powder X-ray diffraction, thermogravimetric analysis, differential scanning calorimetry, X-ray photoelectron spectroscopy, Raman spectroscopy, transmission electron microscopy, atomic force microscopy and scanning electron microscopy.

Graphical Abstract

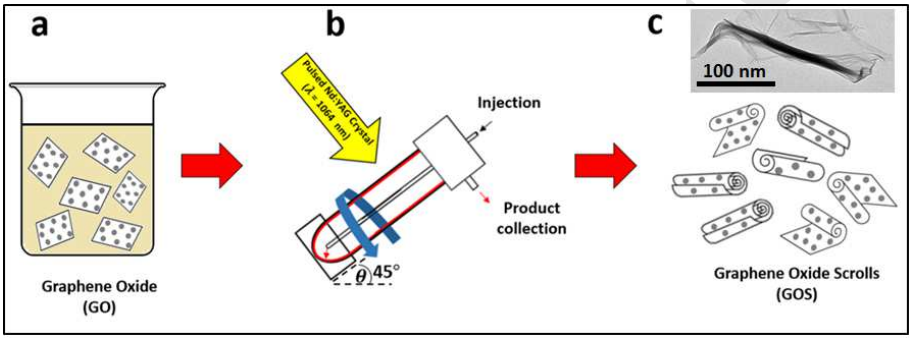

Keywords

Graphene oxide scrolls; Shear stress; Laser irradiation; Vortex fluidics

1. Introduction

In recent years, graphene scrolls have attracted attention as a novel one dimensional (1D) tubular topology materials derived from rolling up a 2D sheet of ubiquitous graphene. Graphene and graphene oxide (GO) scrolls have properties akin to other carbon nano-materials, including high thermal and electrical conductivities and excellent mechanical properties [1,2], with potential in a number of applications. These include hydrogen storage [3,4], supercapacitors [5-7], batteries [8, 9], sensors [10] and electronic devices [11,12]. However, gaining access to graphene scrolls has proved challenging, not only for graphene, but also for graphene oxide and reduced graphene oxide.

Graphene scrolls are accessible directly from graphite using a spinning disc processor (SDP) [13], via sonication of graphite intercalation compounds [14] and from preformed graphene sheets in isopropyl alcohol [15]. Graphene oxide scrolls (GOS) have been prepared from graphene oxide using Lyophilization methods [16], microwave irradiation of graphene oxide [17] and a Langmuir–Blodgett approach, also from preformed graphite oxide [18]. Fabricating such scroll structures from graphene or graphene oxide usually suffers from limitations, including low yield, and using harsh chemicals and energy intensive high temperature and sonication processing, with long processing times. In the present research, we have developed a facile method for the synthesis of GOS from GO sheets in aqueous solution, under high shear stress in a vortex fluidic device (VFD) [19]. This dynamic thin film microfluidic platform has an angled tube rapidly rotating, with the angular dependence important in a number of applications. Within the thin film, typically below ca 500 μm thick, shear stress develops along with pressure waves which can mediate a number of biochemical, chemical and materials transformations [19]. The VFD can be operated in the so called confined mode which is suited for small scale processing, and under continuous flow mode. The latter is an attractive feature of the device for addressing scalability of any processing at the inception of the science. Here jet feeds deliver reagents into the inclined rapidly rotating tube, which is typically a 20 mm OD borosilicate glass or quartz tube.

The VFD is a versatile microfluidic platform with a number of applications, including slicing of single, double and multi-walled carbon nanotubes [20], protein folding [21], enhancing enzymatic reactions [22], protein immobilization [23], fabricating C_{60} tubules using water as an anti-solvent against toluene [24], exfoliation of graphite and boron nitride [25], growth of palladium and platinum nano-particles on carbon nano-onions [26], probing

the structure of self-organized systems, and controlling chemical reactivity and selectivity [27].

In an earlier study we developed the use of a SPD, which by necessity operates under continuous flow, for preparing graphene scrolls directly from graphite, albeit in only 1% yield [13]. The mechanism of this simultaneous exfoliation and scroll formation is understood on a theoretical basis, with a graphene sheet lifting up and bending back under shear, then contacting the upper surface of this graphene sheet, as a stable transition state [13]. Further bending back then leads to spontaneous scroll formation [13]. We hypothesised that GO dispersed in solution has the potential to form scrolls under shear as a shape with the least resistance to shear stress. However, these scrolls will not be packed at the van der Waals limit between carbon atoms between successive turns of the scroll because of the high levels of defects and oxygenation. In contrast, graphene scrolls generated from graphite using a SDP have successive layers of carbon atoms at the van der Waals limit, at distances similar to the distances between layers in graphite itself. We also hypothesised that irradiation of GO under high shear using a pulsed NIR laser may facilitate scroll formation. This is based on the expected increased flexibility of the GO sheets with high induced vibrational energy. There is also potential for a reduction in site defects of the GO on absorption of laser light at 1064 nm, as has been established during slicing of carbon nanotubes in the VFD at the same wavelength [20].

In the present study, we systematically explored the different processing parameter space of the VFD for generating scrolls of GO dispersed in water, along with varying the laser power and the choice of solvent, including isopropyl alcohol (IPA) as a solvent that has been used in forming graphene scrolls [15], and which is environmentally friendly. Further optimization involved recycling the collected solution, but there was little change to the nature of the product (Fig. S6. Supplementary Information).

2. Experimental

2.1. Chemicals and materials

Graphene oxide sheets (GO) (average sheet size: ~ 5 μm in cross section) was synthesized by a modified Hummer's method and purchased from Sigma Aldrich and Carbon Solution, with both product giving similar results.

2.2. Preparation of GOS

The as-received GO was dispersed in water at a number of different concentrations with each solution sonicated for 30 minutes to afford a black stable dispersion, noting that no scrolls were observed after sonication (Fig. 2a-c), prior to processing in the VFD under the described conditions, under a continuous flow rate of 0.45 mL/min in a rotating quartz glass tube 20 mm OD diameter and 18.5 cm long inclined at 45^{o}. Optimal parameters for GOS formation were 4k rpm rotational speed, laser power 250 mJ and 0.2 mg/mL concentration of GO in water. The processing involved delivering a suspension of GO to the hemispherical base of the tube in the VFD with the resulting thin film irradiated by a 5 nanosecond pulsed Q-switch Nd: YAG laser operating at 1064 nm, with an 8 mm diameter laser beam and a repetition rate of 10 Hz.

2.3. Characterization

The GOS were characterized by scanning electron microscopy (SEM) performed using a FEI Quanta 450 High Resolution Field Emission SEM, with a voltage of 10 kV, and working distance of 10 mm, Atomic force microscopy (AFM) – (Nanoscope 8.10 tapping mode), Transmission electron microscopy (TEM) was conducted on a TECNAI 20 microscope operated at 120 and 200 kV. Raman measurements were recorded at an excitation wavelength of 532 nm (≤ 5mW) at room temperature. X-ray powder diffraction (XRD) data were collected using a Bruker Advanced D8 diffractometer (capillary stage) using Cu Kα radiation (λ = 1.5418 Å, 50 kW/40 mA, 2θ = 5 – 80°). Samples for SEM and Raman analysis were prepared on clean silicon wafers. The thermogravimetric analysis (TGA) and differential scanning calorimetry (DSC) measurements were recorded on a Perkin Elmerat operating at a heating rate of 3 C^{o}/min under a nitrogen gas flow. X-ray photoelectron spectroscopy (XPS) data was acquired using a Kratos Axis ULTRA X-ray Photoelectron Spectrometer incorporating a 165 mm hemispherical electron energy analyser. The incident radiation was monochromatic Al Kα X-rays (1486.6 eV) at 150 W (15 kV, 15 ma). Survey (wide) scans were taken at an analyser pass energy of 160 eV and multiplex (narrow) high resolution scans at 20eV. Scanned area is about 0.8 mm x 0.3 mm and the depth is less than 10 nm (volume is approx. 2400 μm^3). Survey scans were carried out over 1200-0 eV binding energy range with 1.0 eV steps and a dwell time of 100 ms. Narrow high-resolution scans were run with 0.05 ev steps and 250 ms dwell time. Base pressure in the analysis chamber was $1.0x10^{-9}$ torr and during sample analysis $1.0x10^{-8}$ torr.

3. Results and discussion

3.1. Optimisation of fabrication of GOS

Details of the processing for transforming 2D GO sheets into 1D tubular like GOS under shear stress within a VFD are summarised in Fig. 1. As received GO was readily dispersed in water as a stable uniform colloidal solution, which is made possible by the hydrophilic groups on the surface of the 2D sheets [6, 18]. Fig. 1a schematically shows flat sheets of GO, before processing in the VFD, with Fig. 1b showing the salient features of the VFD which houses a 20 mm OD diameter quartz tube, 18.5 cm in length, inclined at 45^{o}, which is rapidly rotated with the solution irradiated with a pulsed laser operating at 1064 nm (see below discussions on optimisation studies). Fig. 1c schematically shows partially and fully scrolled GO after processing in the VFD, in accordance with the TEM images (see below).

Establishing the optimum conditions for forming GOS involved systematically exploring the parameter space of the VFD operating under continuous flow. This involved varying the rotational speed from 2k rpm to 8k rpm, followed by using different laser power, 250 mJ, 400 mJ and 600 mJ, at different flow rates of 0.1, 0.45, 1.0 and 1.5 mg/mL, and varying the concentration of GO, 0.1, 0.3 and 0.5 mg/mL. In addition, isopropyl alcohol (IPA), as an alternative solvent which is readily removed in vacuo post processing, was also tested for GOS formation, with GO at 0.2 mg/mL, for different rotational speeds (See Supplementary Information for details**)**. A flow rate of 0.45 mL/min has been established as a good starting point for a number of applications of the VFD with the tube fixed at 45^{o} tilt angle which is the optimal angle for all processing using the VFD [19]. The optimised parameters for the highest conversion to GOS were 4k rpm with the pulsed laser operating at 250 mJ, for an aqueous suspension of GO at 0.2 mg/mL. Under these conditions there is no evidence for residual 2D GO sheets and thus the conversion to GOS or partial GOS is essentially quantitative. Varying these parameters resulted in samples with significantly less GOS and partial GOS, as judged using a number of characterisation techniques (see below).

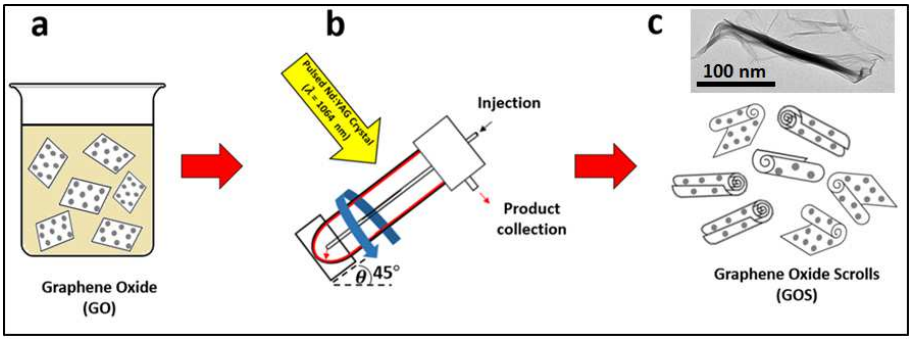

Fig. 1. Schematic illustration of the experimental procedure for fabricating GOS from GO sheets. (a) Solvated GO sheets before processing in the VFD. (b) Schematic of the experimental set up for the vortex fluidic device (VFD) and Nd:YAG pulsed laser irradiation (operating at 1064 nm with the optimised power at 250 mJ) and rotational speed at 4k rpm. (c) GOS after processing in the VFD, inset is TEM image for GOS.

3.2. Characterisation of the GOS

The structure of GOS was initially examined using transmission electron microscopy (TEM), atomic force microscopy (AFM) and scanning electron microscopy (SEM). Fig. 2 shows TEM and AFM images of GO before processing and after VFD processing, establishing the formation of GOS. TEM and AFM images in Fig. 2 a-c are for graphene GO before processing in the VFD, showing the presence of flat surfaces of GO of different sizes, which are one or more layers in thickness, according to the height profiles in Fig. 2d. In addition, TEM and AFM were used to establish the nature of individual scrolls, Fig. 2 e-k. Here the tubular structure of the GOS is revealed, with different diameters ranging from 500 nm to a few micrometres. While the shape of GOS are closely uniform, the differences in diameter presumably reflects the presence of different sizes of GO sheets in the as received material. TEM images establish that the GOS are composed of single scrolled GO sheets, or a relatively low number of graphene oxide layers, which is consistent with direct scrolling of the as received material.

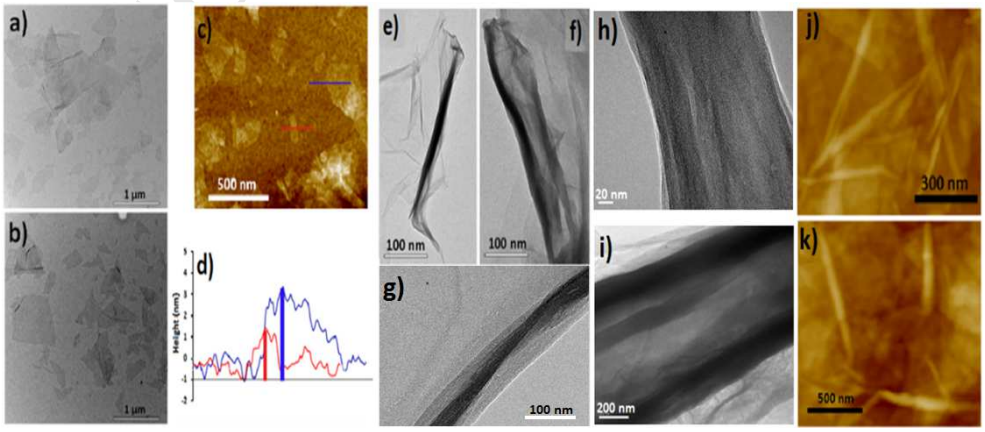

Fig. 2. (a-b) TEM images and (c) AFM images with height profiles in (d) of as-received GO (before processing). (e-i) TEM and (j-k) AFM images of GOS at different magnification after processing in the VFD at 4k rpm rotational speed, tilt angle 45^{o} and a flow rate of 0.45 mL/min, coupled with laser irradiation at 250 mJ.

Further characterisation of the structure of these scrolls used SEM, at different magnification. SEM images of GOS at a low magnification are shown in Fig. 3 a-c, highlighting the uniformity of the GOS material, and thus high conversion of GO to the scrolls. For the optimised speed and concentration now in the absence of laser irradiation, as a control experiment, scroll formation is consistently minimal (Fig. S2 e-f, Supplementary Information). Overall, the results show that GOS of uniform structure are fabricated using the VFD while irradiated with a pulsed laser, at the optimised parameters.

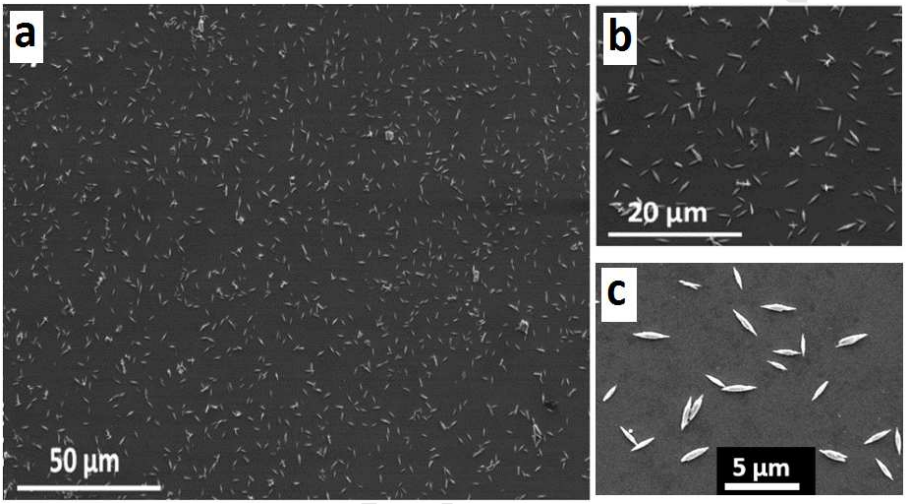

Fig. 3. SEM images of GOS at different magnifications after processing in the VFD at 4k rpm rotational speed, under continuous flow mode, tilt angle 45^{o} and a flow rate of 0.45 mL/min, coupled with laser irradiation at 250 mJ.

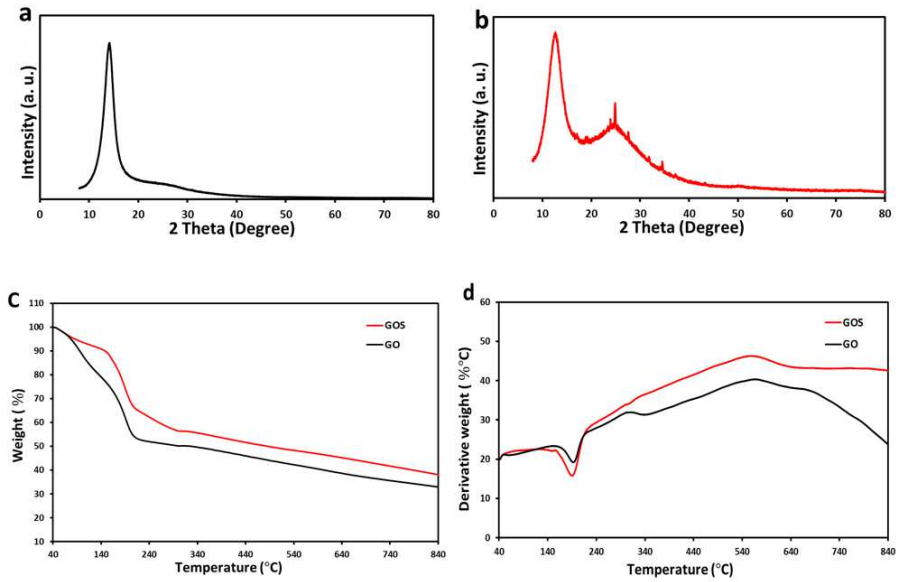

Fig. 4. XRD patterns of (a) as received GO and (b) GOS in the VFD at rotational speed at 4k rpm, under continuous flow mode, tilt angle 45^{o}, with flow rate 0.45 mL/min, coupled with laser irradiation at 250 mJ. (c) TGA and (d) DSC curves of as received GO and GOS at scan rate of 10 °C per minute in a nitrogen atmosphere.

In order to further evaluate the quality of the GOS, x-ray powder diffraction (XRD), thermogravimetric analysis (TGA) and differential scanning calorimetry (DSC) were investigated. Fig. 4a displays XRD for as received GO which has a dominant diffraction peak corresponding to a d-spacing of 8.0818Å, attributed to the (001) plane of the material, as established elsewhere for GO [1, 16]. Fig. 4b reveals that GOS has two peaks, the peak present for as received GO, and another break peak at a d-spacing of 4.15302 Å which is characteristic of the (002) plane, and is consistent with some reduction of the GO in forming the GOS, as noted for laser irradiation of GO in the absence of VFD processing [28, 29].

The TGA of GOS and as received GO, recorded under an atmosphere of nitrogen are shown in Fig. 4c. GO has around 30% mass loss up to150 ◦C and from 160 to 280 ◦C there is a 10% mass loss. This is due to loss of physisorbed water molecules as well as the removal of the oxygen-containing functional groups, as reported in the literature [30]. There is gradual mass loss beyond 250 ◦C, corresponding to further removal of the functional groups [30]. For GOS, there is a mass loss around 28% up to 300 ◦C, which is indicative of removal of some oxygen-containing groups during the VFD processing in the presence of the pulsed laser, and this is consistent with the XPS results (see below). Overall, the mass losses in GOS is lower than that of GO. This is consistent with removal of some of the functional groups during the VFD/laser processing. In this context, we note that processing of CNTs in the VFD while irradiated with a pulsed laser at 1064 nm results in a reduction in the defects along the tubes, presumably with a loss of oxygen functional groups [20]. Fig.4d shows the DSC curves for

GO and GOS, which revealed a narrow exothermic peak at about 196 ℃ for GO, whereas in GOS there is an exothermic peak at 190℃. The results are consistent with some oxygen-containing groups being removed during laser irradiation, analogous to that found in the literatures [30-32].

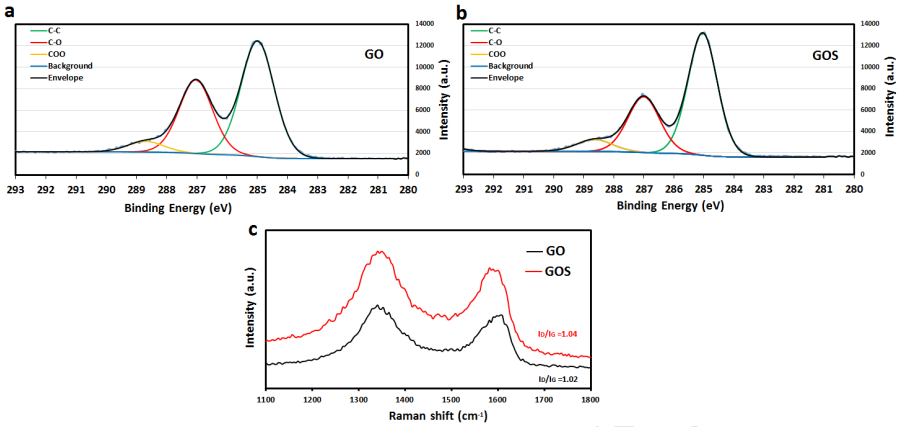

Fig. 5. (a) XPS C 1s spectra of as received GO before VFD processing and (b) GOS formed in the VFD at 4k rpm rotational speed, under continuous mode (flow rate 0.45 mL/min), tilt angle 45^{o} while irradiated with a pulsed laser at 1064 nm and 250 mJ, and (c) Raman spectra of GO and GOS (prepared as for (b)).

In order to further analyse the structure of GOS, Raman spectroscopy and X-ray photoelectron spectroscopy (XPS) were recorded for as received GO and GOS, Fig. 5, along with processing GO in the VFD in the absence of laser irradiation (Fig. S7, Supplementary Information). There is some change in the Raman spectra recorded using a 532 nm excitation laser, from GO to GOS formed in the VFD coupled with the pulsed laser irradiation, Fig. 4c. The D band is a defect-related mode and the G band is associated with the graphitic hexagon-pinch mode [33]. For GO, the G band is at 1600 cm^{-1} which corresponds to ordered sp^2 bonded carbon, and the D band is at 1337 cm^{-1}, which is attributed to edge planes and disordered structures. For GOS, the Raman spectrum shows the presence of G and D bands at 1584 and 1337 cm^{-1}, respectively. It is noteworthy that the position of the G band for GOS is shifted by ≈10 cm^{-1} compared to the as received GO sheets, which is consistent with reduced disorder in the graphitic materials [34, 35]. Analysis of the Raman spectra usually involves a comparison between the ratio of intensity of the G band and D bands. The D/G intensity ratio (ID/ IG) before (GO) and after scroll formation (GOS) are 1.02 and 1.04 respectively, whereas the ratio for processed material in the absence of laser was 1.06. While the difference is not dramatic, the results suggests that in forming GOS, some oxygen functional groups have been removed. This is likely to result in more $\pi-\pi$ interactions [29, 35, 36].

X-ray photoelectron spectroscopy (XPS) was used to determine changes in the oxygen-containing carbonaceous functional groups (C–OH, C–O and COO) associated with VFD processing while irradiated with a pulsed laser. The high resolution XPS C*1s* spectra of GO and GOS are shown in Fig. 4a, b. The amount of C–C component in GO, estimated at ca 57.6 atomic percentage (at%), increased slightly to 60.5 at% in GOS. In addition, the amount of C–O component in GO, estimated at 36.6%, decreased to 30.3% in GOS. The C/O atomic ratio increased from 1.5 for GO to 2 for GOS. The results suggest that some of the oxygen-containing functional groups have been removed during scroll formation in the VFD in the presence of pulsed laser irradiation. More detailed data is presented in Table S1, 2. Supplementary Information. The XPS results are consistent with Raman spectroscopic data, with loss of some oxygen functional groups on forming GOS [29, 37]. XPS was also measured for processed GO in the absence of laser irradiation, with the C–C component estimated at 57.9% which is almost the same as the starting material, while the C–O component was estimated at 33.0 % which is less than that the 36.6% for as received GO (Table S1, 3. Supplementary Information).

The formation of GOS from GO sheets arises from the shear stress in the complex fluid dynamics in the thin film in the VFD [19]. At 45^{o} tilt angle, the liquid is accelerated up the tube and pulled down by gravity, and there are rotational speed induced pressure waves [19-22]. Coupling shear and pressure waves with induced vibrational energy in the GO sheets upon laser irradiation presumably facilitates the formation of the scrolls. Moreover, it would account for no further improvement in the degree of scrolling for each GO sheet upon recycling the colloidal suspension of the GOS back through the VFD at the optimised processing parameters, at the same pressure waves present at 4k rpm. We note that in an earlier study the VFD was used to exfoliate graphite into single layer graphene sheets without the formation of any scrolls [19], in the absence of laser irradiation. Thus any loss of oxygen functionality at the edge of the GO sheets in the present study, under optimised VFD processing and laser irradiation is unlikely to facilitate scroll formation.

4. Conclusion

We have established an essentially quantitative formation of GOS directly from GO in water in a VFD microfluidic thin film processing platform while irradiated with a NIR pulsed laser, with the product devoid of 2D GO sheets. Importantly the processing is under continuous flow such that it can be scaled up, limited by the volume that can be delivered

through a single VFD unit for a concentration of 0.2 mg/mL. Scale up beyond this is possible for a number of VFD units operating in parallel or in a single large VFD. The versatility of the VFD is further highlighted with this new application of the device, with the operating parameters readily systematically varied in arriving at the optimised settings, under continuous flow. The residence time of liquid entering the VFD and exiting at the top of the rotating tube is close to 11 minutes for a flow rate of 0.45 mL/min, such that the processing time for small volumes of water containing dispersions of GOS is short. This new strategy for generating GOS on demand, with the ability to scale up under continuous flow sets the scene for developing the applications of GOS, with synthetically useful quantities ca. 50 mg being readily prepared in a single VFD.

Acknowledgment

T.M.D.A. thanks Taibah University (Ministry of Education, Saudi Arabia) for funding his scholarship. The authors thank support of this work by the Australian Research Council, the Government of South Australia, and thanks the Australian Microscopy & Microanalysis Research Facility (AMMRF) and the Australian National Fabrication Facility (ANFF) for accessing microscopic facilities.

References

[1] Y. Yang, X. Zhang, H. Wang, H. Tang, L. Xu, H. Li, et al., Preparation of Nanoscrolls by Rolling up Graphene Oxide–Polydopamine–Au Sheets using Lyophilization Method, Chemistry–An Asian Journal 11 (2016) 1821-1827.
[2] X. Wang, D.-P. Yang, G. Huang, P. Huang, G. Shen, S. Guo, et al., Rolling up graphene oxide sheets into micro/nanoscrolls by nanoparticle aggregation, Journal of Materials Chemistry 22 (2012) 17441-17444.
[3] X. Shi, N.M. Pugno, H. Gao, Mechanics of carbon nanoscrolls: a review, Acta Mechanica Solida Sinica 23 (2010) 484-497.
[4] G. Mpourmpakis, E. Tylianakis, G.E. Froudakis, Carbon nanoscrolls: a promising material for hydrogen storage, Nano letters 7 (2007) 1893-1897.
[5] F. Zeng, Y. Kuang, G. Liu, R. Liu, Z. Huang, C. Fu, et al., Supercapacitors based on high-quality graphene scrolls, Nanoscale 4 (2012) 3997-4001.
[6] T. Fan, W. Zeng, Q. Niu, S. Tong, K. Cai, Y. Liu, et al., Fabrication of high-quality graphene oxide nanoscrolls and application in supercapacitor, Nanoscale research letters 10 (2015) 192.
[7] W. Zhou, J. Liu, T. Chen, K.S. Tan, X. Jia, Z. Luo, et al., Fabrication of Co 3 O 4-reduced graphene oxide scrolls for high-performance supercapacitor electrodes, Physical Chemistry Chemical Physics 13 (2011) 14462-14465.

[8] M. Yan, F. Wang, C. Han, X. Ma, X. Xu, Q. An, et al., Nanowire templated semihollow bicontinuous graphene scrolls: designed construction, mechanism, and enhanced energy storage performance, Journal of the American Chemical Society 135 (2013) 18176-18182.
[9] X. Li, Y. Zhang, T. Li, Q. Zhong, H. Li, J. Huang, Graphene nanoscrolls encapsulated TiO 2 (B) nanowires for lithium storage, Journal of Power Sources 268 (2014) 372-378.
[10] H. Li, J. Wu, X. Qi, Q. He, C. Liusman, G. Lu, et al., Graphene oxide scrolls on hydrophobic substrates fabricated by molecular combing and their application in gas sensing, Small 9 (2013) 382-386.
[11] T. Sharifi, E. Gracia-Espino, H.R. Barzegar, X. Jia, F. Nitze, G. Hu, et al., Formation of nitrogen-doped graphene nanoscrolls by adsorption of magnetic γ-Fe2O3 nanoparticles, Nature communications 4 (2013) 2319.
[12] K. Feng, B. Tang, P. Wu, “Evaporating” graphene oxide sheets (GOSs) for rolled up GOSs and its applications in proton exchange membrane fuel cell, ACS applied materials & interfaces 5 (2013) 1481-1488.
[13] X. Chen, R.A. Boulos, J.F. Dobson, C.L. Raston, Shear induced formation of carbon and boron nitride nano-scrolls, Nanoscale 5 (2013) 498-502.
[14] M.V. Savoskin, V.N. Mochalin, A.P. Yaroshenko, N.I. Lazareva, T.E. Konstantinova, I.V. Barsukov, et al., Carbon nanoscrolls produced from acceptor-type graphite intercalation compounds, Carbon 45 (2007) 2797-2800.
[15] X. Xie, L. Ju, X. Feng, Y. Sun, R. Zhou, K. Liu, et al., Controlled fabrication of high-quality carbon nanoscrolls from monolayer graphene, Nano letters 9 (2009) 2565-2570.
[16] Z. Xu, B. Zheng, J. Chen, C. Gao, Highly efficient synthesis of neat graphene nanoscrolls from graphene oxide by well-controlled lyophilization, Chemistry of Materials 26 (2014) 6811-6818.
[17] M. Quintana, M. Grzelczak, K. Spyrou, M. Calvaresi, S. Bals, B. Kooi, et al., A simple road for the transformation of few-layer graphene into MWNTs, Journal of the American Chemical Society 134 (2012) 13310-13315.
[18] Y. Gao, X. Chen, H. Xu, Y. Zou, R. Gu, M. Xu, et al., Highly-efficient fabrication of nanoscrolls from functionalized graphene oxide by Langmuir–Blodgett method, Carbon 48 (2010) 4475-4482.
[19] J. Britton, K.A. Stubbs, G.A. Weiss, C.L. Raston, Vortex Fluidic Chemical Transformations, Chemistry-A European Journal (2017).
[20] K. Vimalanathan, J.R. Gascooke, I. Suarez-Martinez, N.A. Marks, H. Kumari, C.J. Garvey, et al., Fluid dynamic lateral slicing of high tensile strength carbon nanotubes, Scientific Reports 6 (2016) 22865.
[21] T.Z. Yuan, C.F.G. Ormonde, S.T. Kudlacek, S. Kunche, J.N. Smith, W.A. Brown, et al., Shear-Stress-Mediated Refolding of Proteins from Aggregates and Inclusion Bodies, ChemBioChem 16 (2015) 393-396
[22] J. Britton, L.M. Meneghini, C.L. Raston, G.A. Weiss, Accelerating Enzymatic Catalysis Using Vortex Fluidics, Angewandte Chemie 128 (2016) 11559-11563.
[23] J. Britton, C.L. Raston, G.A. Weiss, Rapid protein immobilization for thin film continuous flow biocatalysis, Chemical Communications 52 (2016) 10159-10162.
[24] K. Vimalanathan, R.G. Shrestha, Z. Zhang, J. Zou, T. Nakayama, C.L. Raston, Surfactant-free Fabrication of Fullerene C_{60} Nanotubules Under Shear, Angewandte Chemie International Edition (2016).
[25] X. Chen, J.F. Dobson, C.L. Raston, Vortex fluidic exfoliation of graphite and boron nitride, Chemical Communications 48 (2012) 3703-3705.

[26] F.M. Yasin, R.A. Boulos, B.Y. Hong, A. Cornejo, K.S. Iyer, L. Gao, et al., Microfluidic size selective growth of palladium nano-particles on carbon nano-onions, Chemical Communications 48 (2012) 10102-10104.
[27] L. Yasmin, X. Chen, K.A. Stubbs, C.L. Raston, Optimising a vortex fluidic device for controlling chemical reactivity and selectivity, Scientific reports 3 (2013).
[28] Z. Bo, X. Shuai, S. Mao, H. Yang, J. Qian, J. Chen, et al., Green preparation of reduced graphene oxide for sensing and energy storage applications, Scientific reports 4 (2014).
[29] L. Huang, Y. Liu, L.-C. Ji, Y.-Q. Xie, T. Wang, W.-Z. Shi, Pulsed laser assisted reduction of graphene oxide, Carbon 49 (2011) 2431-2436.
[30] C. Zhang, M. Chen, X. Xu, L. Zhang, L. Zhang, F. Xia, et al., Graphene oxide reduced and modified by environmentally friendly glycylglycine and its excellent catalytic performance, Nanotechnology 25 (2014) 135707.
[31] H. Li, G. Zhu, Z.-H. Liu, Z. Yang, Z. Wang, Fabrication of a hybrid graphene/layered double hydroxide material, Carbon 48 (2010) 4391-4396.
[32] J. Wu, X. Shen, L. Jiang, K. Wang, K. Chen, Solvothermal synthesis and characterization of sandwich-like graphene/ZnO nanocomposites, Applied Surface Science 256 (2010) 2826-2830.
[33] M.S. Dresselhaus, G. Dresselhaus, R. Saito, A. Jorio, Raman spectroscopy of carbon nanotubes, Physics reports 409 (2005) 47-99.
[34] A.C. Ferrari, J. Robertson, Interpretation of Raman spectra of disordered and amorphous carbon, Physical review B 61 (2000) 14095.
[35] C.A. Amadei, I.Y. Stein, G.J. Silverberg, B.L. Wardle, C.D. Vecitis, Fabrication and morphology tuning of graphene oxide nanoscrolls, Nanoscale 8 (2016) 6783-6791.
[36] D.H. Suh, Formation of hexagonal boron nitride nanoscrolls induced by inclusion and exclusion of self-assembling molecules in solution process, Nanoscale 6 (2014) 5686-5690.
[37] S. Evlashin, P. Dyakonov, R. Khmelnitsky, S. Dagesyan, A. Klokov, A. Sharkov, et al., Controllable Laser Reduction of Graphene Oxide Films for Photoelectronic Applications, ACS applied materials & interfaces 8 (2016) 28880-28887.